478 EVOLVING GEOMETRIES IN THE PRECIPITATION PATTERNS OF 2004-2012 U.S. LANDFALLING HURRICANES[1]

Stephanie E. Zick* and Corene J. Matyas
University of Florida, Gainesville, FL

1. INTRODUCTION

Tropical cyclones (TCs) occur annually in every ocean basin in the Northern Hemisphere (Gray 1968), bringing dangerous winds, storm surges, and precipitation to coastal and inland regions, many of which are heavily populated and especially vulnerable to these weather phenomena. In considering TC precipitation forecasts, numerous factors modulate the distribution of convection during landfall, including storm size, storm morphology, storm motion, topography and land cover, vertical wind shear, and interaction with midlatitude synoptic and mesoscale features (Rogers et al. 2009). In forecast settings, TC precipitation is an enormous operational challenge that needs to be addressed through coordination between researchers and forecasters (Elsberry 2002). Consequently, Rappaport et al. (2009) list improvements to TC precipitation forecasts among the most important research challenges for tropical meteorologists.

In this study, we formulate of a suite of shape metrics to quantify the evolution of TC precipitation. Shape is a fundamental aspect of spatial analysis in geography research (MacEachren 1985; Wentz 1997). Here, we use the term *shape* to refer to the two-dimensional extent of a geometric feature as adopted by (Li et al. 2013), rather than a one-dimensional linear feature (e.g., TC track) or a three-dimensional volumetric feature (e.g., TC convection). A *shape metric* assigns a mathematical quantity to the two-dimensional feature, thus extending a qualitative description of shape to an objective and reproducible mathematical quantity.

Arguably, the most successful application of shape analysis in meteorology is the Dvorak technique (Dvorak 1975; Velden et al. 1998) for estimating TC intensity using cloud patterns in satellite imagery. In a review of the success of this method, (Knaff et al. 2010) found that half (three-quarters) of Dvorak estimates are within 3 (6) m s^{-1} of the best track intensities. However, a major limitation of Dvorak is it was not designed for systems undergoing extratropical transition (ET), which occurs in 46 percent of Atlantic TCs (Hart and Evans 2001) upon exiting the tropics and interacting with mid-latitude frontal regions. Although a strict definition of ET is yet to be agreed upon (Malmquist 1999), the theoretical process involves a structural reorganization from a compact symmetric system driven by latent heating in its warm inner core to an asymmetric, comma-shaped system driven by the temperature gradient between the tropics and poles (DiMego and Bosart 1982; Foley and Hanstrum 1994; Hart and Evans 2001; Jones et al. 2003).

The present study represents an advancement upon previous work by Matyas (2007, 2008, 2009) toward the development of effective shape metrics for studying evolving TC precipitation patterns. Based on previous research on the evolution of TC structure during weakening, landfall, and ET, we expect that the storm structure will transition from shapes characteristic of mature hurricanes (circular, cohesive, centralized) to shapes characteristics of non-tropical or dissipating storms (asymmetric, fragmented, and dispersed). In this article, we demonstrate how shape metrics may be used to assess (a) the overall evolution of and (b) the spatiotemporal positions of significant changes to TC precipitation structure. The final goal is to apply these shape metrics in operational meteorology forecast settings towards improved rainfall forecasts.

2. DATA

This research utilizes 3-hourly accumulated precipitation from the North American Regional Reanalysis (NARR), which is documented in Mesinger et al. (2006). The NARR is a model-data assimilation system produced by the National Centers for Environmental Prediction/National Center for Atmospheric Research (NCEP/NCAR). Output is provided on a 32 km x 32 km Lambert Conformal conic equal area projection. Since all pixels are equivalent in geographic area and may be weighted evenly, this projection is ideal for image analysis.

The NARR was developed for hydrometeorology and hydroclimatology research (Mesinger et al. 2006). Through assimilation of hourly precipitation, the model more accurately characterizes observed precipitation

* *Corresponding author address*: Stephanie E. Zick, Univ. of Florida, Dept. of Geography, Gainesville, FL 32611-7315; e-mail: sezick@ufl.edu.

1: This work is part of a study currently under peer review by the *Annals of the Association of American Geographers* (Zick and Matyas 2016).

distributions compared with previous reanalysis systems (Mesinger et al. 2006; Bukovsky and Karoly 2007; Becker et al. 2009). Precipitation observations are not assimilated directly but through an indirect nudging technique that modifies the atmospheric latent heating profile (Lin et al. 1999). The resulting hydrologic cycle is significantly improved. Thus, the NARR is recommended for water budget and dynamic process studies (Ruane 2010a,b). Despite these favorable recommendations, there are limitations to the dataset including a tendency to over- (under-) estimate light (heavy) precipitation (Becker et al. 2009; Zick and Matyas 2015a) and a warm bias in the lower troposphere (Royer and Poirier 2010). However, research shows that precipitation assimilation over the ocean in the vicinity of TCs after 2004 leads to an improved representation of the large-scale TC structure (Zick and Matyas 2015a). Therefore, in the 2004-2012 period, this dataset provides a robust representation of the spatial configuration of moderate (1-10 mm hr^{-1}) precipitation, even though higher rain rates may be underestimated.

Consistent with research into the depiction of TCs within the NARR (Zick and Matyas 2015a,b), we limit this research to the 36 U.S. landfalling storms with tropical storm intensity (17 ms^{-1}) or greater during the 2004-2012 North Atlantic hurricane seasons (Figure 1). Additionally, due to degraded representation of TCs over the remote tropical oceans (Schenkel and Hart 2012; Zick and Matyas 2015b), we consider only portions of the TC life cycle when the center is within 10° latitude/longitude of the U.S. coastline where higher-quality and more abundant observations are available to the data assimilation system (Figure 1). The TC center positions and intensities are taken from the National Hurricane Center (NHC)'s Best Track (BT) dataset. These 6-hourly post-analysis positions provide the most accurate estimates currently available for TC position and intensity (Jarvinen 1984; Elms et al. 1993). The NHC also provides the timing/location of landfall and maximum intensity in its TC reports. Following Jagger and Elsner (2006), TC positions are interpolated to 3-hourly using a spline interpolation.

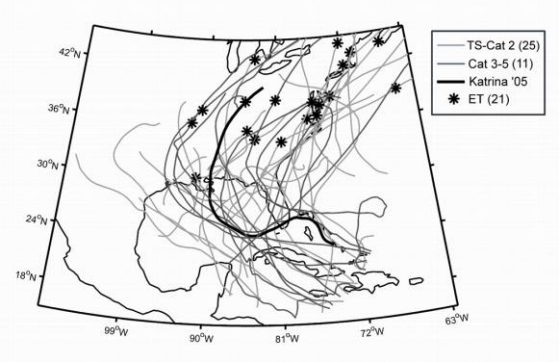

Figure 1 2004-2012 U.S. landfalling tropical cyclone tracks (subset by maximum intensity) and the time of extratropical transition (ET), if applicable.

3. METHODS

3.1 Delineation of TC Precipitation

To quantify the shape of the precipitation pattern, we must first construct a binary image (Figure 2). Precipitation within 600 km from the TC center is retained as TC-associated precipitation. A minimum threshold is required to delineate the precipitation region. Due to the nature of precipitation processes, there are large areas of zero and light precipitation (<1 mm hr^{-1}) producing a distribution that is strongly non-Gaussian. Therefore, we use a minimum precipitation threshold that is based on the greatest 90th percentile of precipitation values observed within the 600 km radius (Figure 2). In applying this definition, rain rate thresholds range from near zero (in weak and dissipating TCs) to 7.67 mm hr^{-1} with a mean (median) of 1.80 (1.43) mm hr^{-1}. Finally, only objects with a minimum of 10 pixels (10,240 km^2 in area) are included.

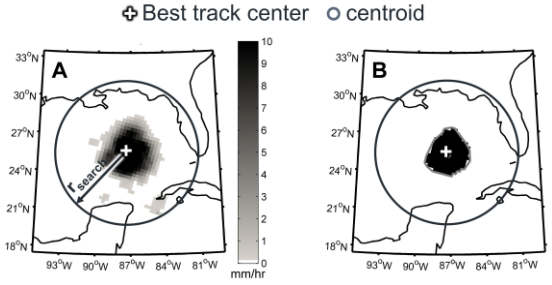

Figure 2 Example of shape delineation based on (left) NARR 3-hour mean precipitation rate within r = 600 km search radius with the corresponding (right) binary precipitation cluster(s) and associated centroids and convex hulls.

3.2 Shape Metrics

Compactness of shape was first conceived in 1822 by Carl Ritter (Frolov 1975) and its measurement has been summarized by previous researchers (MacEachren 1985; Li et al. 2014). The shape metrics developed in this section represent numerical evaluations of a specialized aspect of shape—compactness. TC precipitation is highly symmetric and centrally organized in intense tropical systems. As a TC transitions from a warm core to an extratropical system, or as the TC dissipates, the weather system loses its characteristic central, symmetric qualities (Figure 3). In fact, TCs that undergo ET often assume a triangular or "delta-shaped" precipitation pattern that is displaced to the north of the storm's circulation center (Shimazu 1998; Klein et al. 2000). Thus, compactness measures are ideal quantities for consideration.

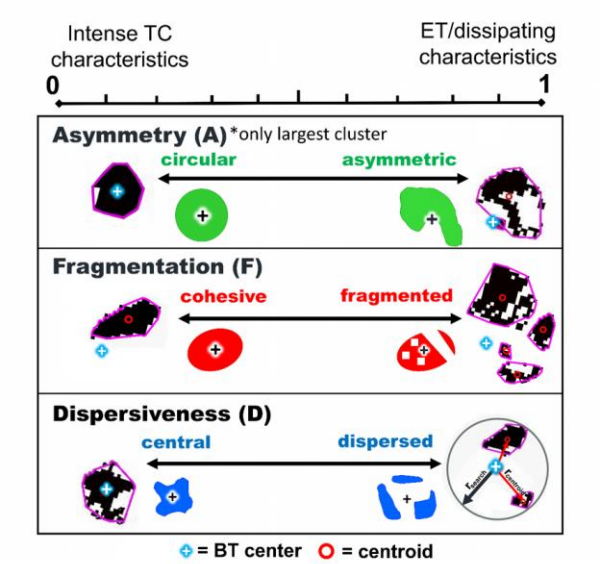

Figure 3 Summary of asymmetry, fragmentation, and dispersiveness shape metrics.

We formulate three shape metrics that encompass characteristic geometries of TCs moving into the mid-latitudes: asymmetry (A), fragmentation (F), and dispersiveness (D). In defining these metrics, we utilize the following simple geometrical concepts (Table 1): 1) a centroid, 2) a convex hull, 3) the perimeter of the convex hull, 4) the solid area of the cluster, 5) the area enclosed by the convex hull, and 6) the number of distinct or isolated structures within the 600 km search radius. Spatial patterns are quantified every 3 hours.

Table 1. Important Geometric Parameters for the Computation of Shape Metrics

Geometric Parameter	Definition
Centroid	Geographic center of mass of the region
Convex Hull	Smallest convex polygon that can contain the region
Perimeter	Distance around the boundary of the region
Area	Actual area of the region
Convex Area	Area of the smallest convex polygon that can contain the region

Asymmetry (A): A circle is the most compact two-dimensional shape (Schwartzberg 1965; Angel et al. 2010; AghaKouchak et al. 2011). Following from this fundamental concept is the area to perimeter ratio (APR), which is essentially a measure of circularity, which ranges from 0 (non-circular) to 1 (circular). To measure asymmetry as opposed to circularity, this metric is calculated as 1 minus the squared APR (Equation 1). A size modification is necessary to avoid scoring small precipitation clusters at or near the same level as large clusters, which are often major hurricanes (winds > 50 m s^{-1}). Furthermore, only the largest cluster of pixels is considered in the asymmetry metric. In the final measure (Equation 1), large and circular precipitations structures score lower (more symmetric) on the scale compared with small and/or asymmetric precipitation structures.

$$A = 1 - \frac{4\pi \times Area}{Perim^2}\left(\frac{\log_{10} Area}{\log_{10} \pi r_{search}^2}\right) \quad (1)$$

Fragmentation (F): The fragmentation shape metric is related to the connectivity index from AghaKouchak et al. (2011) with two major modifications. First, a more stringent penalizing factor is applied as the precipitation splinters from one cluster into additional isolated clusters. Second, fragmentation is scaled by the spatial pattern's solidity, which represents the proportion of the convex area that is filled with nonzero pixels. Collectively, we calculate the final fragmentation index as the product of solidity (summed over all clusters) and the modified connectivity. As with asymmetry, the solidity-connectivity product is subtracted from one (Equation 2) to arrive at a final shape metric that ranges from 0 (cohesive) to 1 (fragmented) (Figure 3).

$$F = 1 - \sum_{i=1}^{NC} \frac{Area_i}{ConvexArea_i}\left[1 - \frac{NC - 1}{NC + \log_{10} Area}\right] \quad (2)$$

Dispersiveness (D): The last shape metric, dispersiveness (D), measures the spread of the centers of precipitation clusters away from the TC circulation center. The ratio of the centroid radius ($r_{centroid}$) to the search radius (r_{search} = 600 km) is a measure of dispersion. When precipitation fragments into multiple clusters, the dispersion is calculated individually for each centroid, and the values are summed. The final dispersiveness metric also includes a weighting factor so that larger clusters contribute more strongly to the final quantity (Equation 3).

$$D = \sum_{i=1}^{NC} \frac{Area_i}{\sum_j^{NC} Area_j}\left(\frac{r_{centroid,i}}{r_{search}}\right) \quad (3)$$

Moving Mann-Whitney *U* test: Rather than subjectively determining the time period when precipitation is evolving, we use a sliding window to split the time series into two equal length samples and perform a two-sided Wilcoxon rank sum test (Wilcoxon 1945), also known as a Mann-Whitney *U* test. This nonparametric statistical test compares the distributions of two samples via changes in the median. The null hypothesis is that the two samples are drawn from an identical continuous distribution. When $p < 0.05$, the test indicates an evolving precipitation structure with a 95% confidence level. Multiple sample sizes for the moving window are considered with little variation in the results for sample sizes larger than five and less than ten. For the reported results, we select a sample size of seven.

4. RESULTS

4.1 A case study of Hurricane Katrina (2005)

In this section, the methods are applied toward understanding the spatial evolution of precipitation in Hurricane Katrina (2005) (Figure 4). This case study demonstrates how the evolving precipitation geometry is related to internal structural changes and interactions with the large-scale environment. There have been a plethora of modeling (Jin et al. 2008; Torn and Hakim 2009; Abarca and Corbosiero 2011) and observational (McTaggart-Cowan et al. 2007; Hence and Houze 2008; Didlake and Houze 2009) studies of Katrina, but these primarily examined mesoscale processes in the eyewall and rainbands. In contrast, our method focuses on the storm-scale precipitation structure.

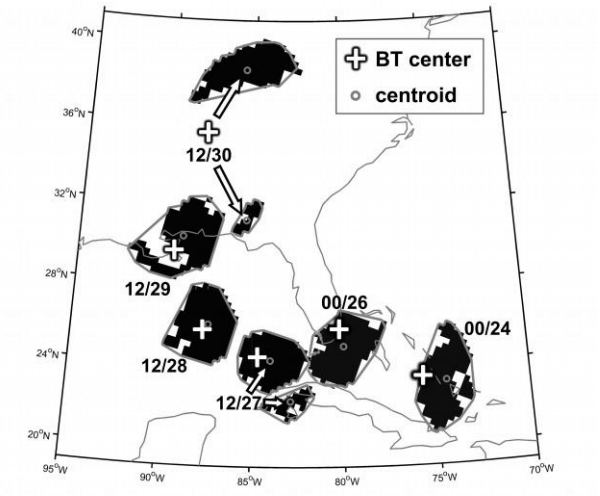

Figure 4 Synoptic evolution of NARR precipitation > 90th percentile threshold. Convex hulls are outlined for each shape in gray for the corresponding time (hour/day)

Figure 1 shows the BT track for Hurricane Katrina in bold. Forecasters at the NHC designated the storm as a tropical depression over the southeastern Bahamas at 1800 UTC August 23 (18/23, Figure 5A) (Knabb et al. 2005). It is important to note the stochastic quality of the shape metric time series (Figure 5B). This is partially related to the nature of TC convection (e.g., (Simpson et al. 1997) but also a non-physical artifact that arises from objectively delineating a binary image. Thus, we apply a 6-hour running mean for the remaining results.

During the storm's lifecycle, the moving Mann-Whitney *U* test (Figure 5C,6) reveals five periods (EV1-5) of precipitation evolution, as indicated by $p < 0.05$ for one or more shape metrics:

(1) EV1: Early in the lifecycle of Katrina, the shape metrics (Figure 5B) indicate a central but slightly asymmetric structure with low fragmentation. As the storm intensified (Figure 5A), dispersiveness and asymmetry decrease (Figure 5B), which we expect for a developing TC since persistent inner core convection is required to spin-up a warm core system (Hendricks et al. 2004). However, fragmentation increases during this time because the system was battling dry air entrainment (Knabb et al. 2005), which slowed the initial intensification.

(2) EV2: The second restructuring period is around the time of landfall at 2230 UTC 25 August over Miami, Florida as a category 1 hurricane. McTaggart-Cowan et al. (2007) and NHC forecasters (Knabb et al. 2005) report the establishment of a complete eyewall in the 12 hours before landfall. Accordingly, fragmentation (Figure 5B) decreases during this time. Hurricane Katrina showed only minor signs of weakening as it crossed over the moisture-rich southern Florida Everglades, and there is no evidence of loss of structure (Figure 6). During this 6-hour period, however, convection was displaced south of the eye (Figure 4) due to northerly wind shear, resulting in moderate values of asymmetry and increasing dispersiveness (Figure 5B-C,6C).

(3) EV3: A third evolutionary period occurs between 0900 and 1800 UTC on 27 August and corresponds to significant increases in symmetry, cohesiveness, and centeredness (Figures 5,6). After crossing the Florida peninsula, Katrina emerged into a conducive synoptic environment for intensification due to low vertical wind shear, favorable upper-level divergence, and anomalously warm sea surface temperatures (SSTs) in the eastern Gulf of Mexico. Intensification proceeded as two periods of rapid intensification (RI: winds increase by > 30 knots, or 15.4 m s^{-1}, in 24 hours as defined by Kaplan and DeMaria 2003), with the shape metrics indicating significant structural reorganization beginning at the end of the first RI period (Figures 5,6). During this restructuring, a large eye became visible on satellite imagery and the radius of tropical storm-force winds nearly doubled in size (Knabb et al. 2005). Since asymmetry is the only metric that depends on size, Mann-Whitney *U* test results (Figures 5,6) suggest that reorganization was only partially due to an increase in horizontal scale. The precipitation pattern also becomes increasingly cohesive and centrally organized (Figures 5B,6B-C). EV3 is quickly followed by the second RI, with the TC reaching a final peak intensity of 77 m s^{-1} (902 hPa) at 1800 UTC 28 August.

(4) EV4: A fourth reorganization occurs during an approximately 24-hour period beginning 1200 UTC 28 August, or 6 (24) hours prior to the timing of peak intensity (landfall). At this time, intensification leveled off and all shape metrics reach a minima (Figure 5), indicating the highest degree of compactness attained during the storm's lifetime. Positioned just 315 km from the Louisiana coastline, Hurricane Katrina was one of the largest and strongest TCs in recorded history in the North Atlantic basin (Knabb et al. 2005). Although TCs do not usually maintain these intensities for long time periods, there were no detrimental environmental conditions (e.g.

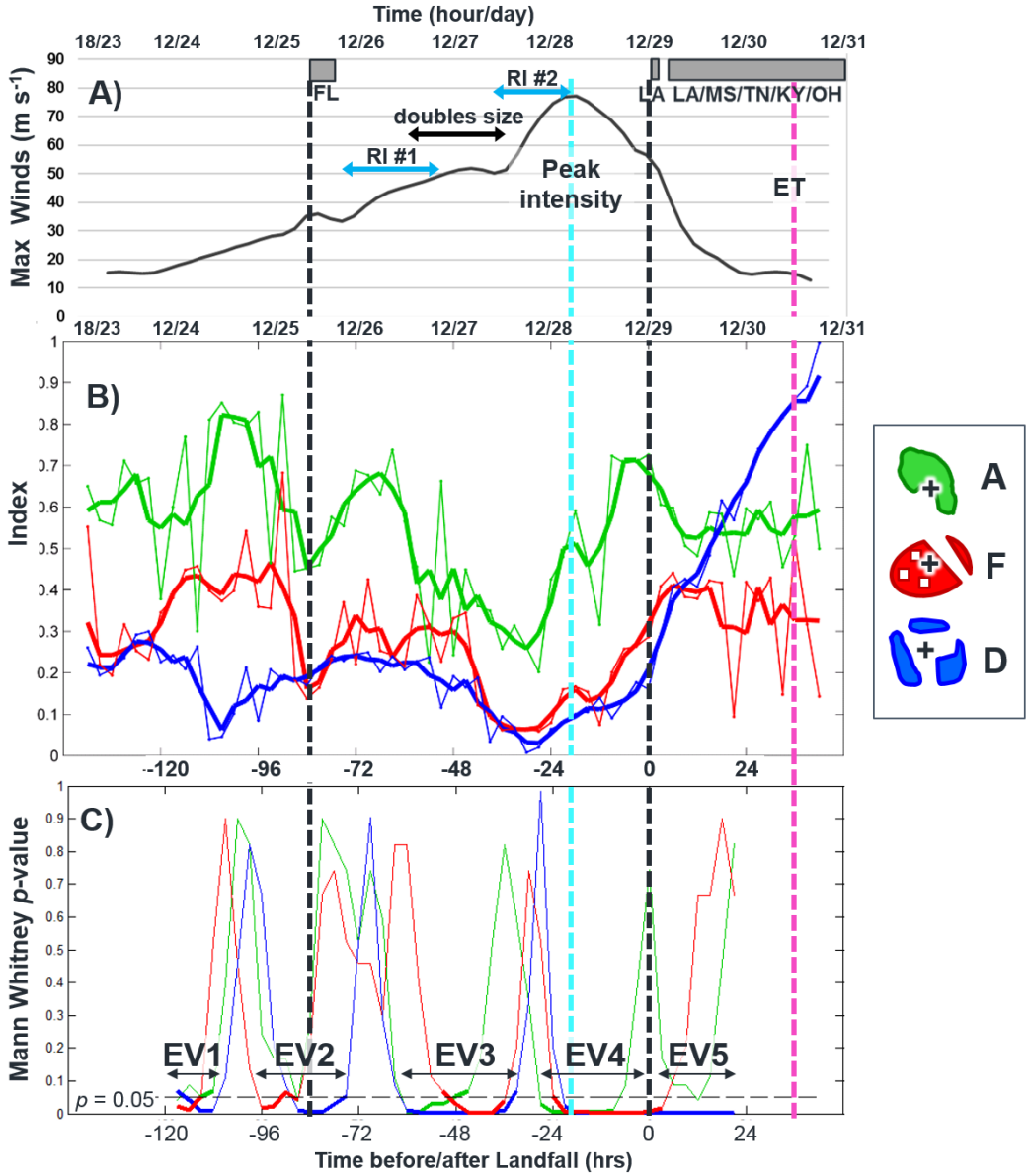

Figure 5 Time series of (A) intensity, (B) shape metrics, and (C) Mann-Whitney U test p-values for Hurricane Katrina (2005). For the shape metrics, a 6-hour running mean (bold) is applied to the 3-hourly quantities (light). Times of peak intensity, landfall, and extratropical transition (ET) are designated with cyan, black, and pink dashed lines, respectively.

low SSTs or high wind shear) to suggest weakening, and the NHC forecast was for the storm to weaken only slightly before landfall. Yet, the shape metric quantities begin to increase before the storm reached peak intensity (Figures 5,6). The fourth restructuring corresponds to a period in which precipitation is eroded on the northwestern semi-circle (Figure 5), potentially indicating that dry air was limiting convection in the outer rainbands. Additionally, dry air wrapped cyclonically inward (Figure 4) and the western and southern eyewall convection was suppressed during the final approach to landfall. The delay between the shape metric minima and the peak intensity may be explained by the fact that dry air must enter the system at the periphery and become entrained cyclonically inward to penetrate the inner core and impact peak winds in the eyewall (Riemer and Montgomery 2011). In this case, the erosion of precipitation in the NW quadrant precedes weakening by about 6-9 hours.

However, additional cases should be examined to determine if the timing for dry air impacts in Katrina is representative the timing of dry air entrainment impacts.

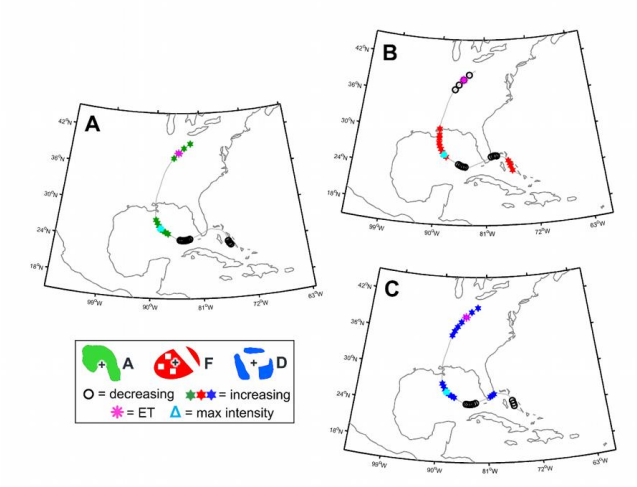

Figure 6 Along-track placement of times steps for Hurricane Katrina (2005) when moving Mann-Whitney U test indicates an evolving precipitation structure with $p < 0.05$.

(5) EV5: The final restructuring occurs prior to and during ET. During this process, the system continues to show significant increases in dispersiveness, while fragmentation and asymmetry begin to decrease. This ET process and its relation to shape metric evolution is examined further in Zick and Matyas (2016, in review).

4.2 All 2014-2012 TCs

We now apply this shape metric methodology to the entire set of 2004-2012 U.S. landfalling TCs. Although the three shape metrics are measures of compactness, Pearson's correlation coefficients among the metrics reveal weak to moderate relationships (Table 2). Asymmetry and fragmentation are the most closely correlated (r = 0.48), while asymmetry and dispersiveness are only weakly correlated (r = 0.093).

Table 2 Pearson's correlation coefficients among shape metrics and between each shape metric and TC intensity (as measured by maximum sustained wind speed). All correlations are significant at confidence levels greater than 99%.

Shape metric/TC intensity	A	F	D
Asymmetry (A)	--		
Fragmentation (F)	0.48	--	
Dispersiveness (D)	0.093	0.32	--
TC intensity	-0.20	-0.32	-0.60

Thus, as demonstrated in the Katrina case study, the three shape metrics reveal unique, although not entirely independent, aspects of TC rainfall pattern changes. Generally, major hurricanes are more compact than tropical storms and weak hurricanes, as indicated by the negative correlations between each shape metric and the TC intensity measured by maximum sustained wind speed (Table 2, Figure 7). Dispersiveness displays the strongest negative correlation with intensity. Additionally, this metric spans the entire range of [0,1], whereas asymmetry and fragmentation span smaller subsets of approximately [0.2,0.85] and [0,0.7], respectively (Figure 7). Nonetheless, these correlations are robust ($p < 0.05$) for all three shape metrics. We expect some variance due to environmental factors, such as storm motion and weak vertical wind shear (e.g., Chen et al. 2006), that lead to asymmetries but do not necessarily TC intensity.

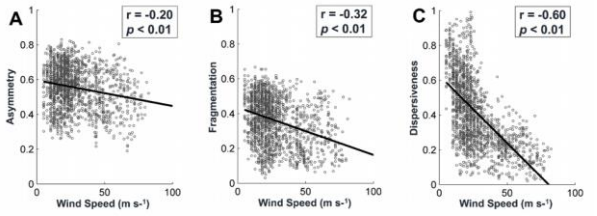

Figure 7 Scatter plots of (A) asymmetry, (B) fragmentation, and (C) dispersiveness 6-hour running mean indices versus TC intensity, as represented by Best Track maximum sustained wind speed (in m s^{-1}) for all n=1712 positions. Least squares regression lines are overlain in black

In Figure 8, we display the average overall shape metric trends on a latitude-longitude grid, constructed with the requirements of ≥ 2 TCs and ≥ 5 significant ($p <$ 0.05) data points for the average shape metric trend to be plotted. Generally, we observe increasing symmetry, cohesiveness, and central structure as TCs enter the southern and southeastern Gulf of Mexico (to the northwest of Cuba). Increasing compactness in this region may be partially related to intensification as TCs move over the Loop Current (and the associated above average SSTs) after land interaction with Florida and/or the Greater Antilles islands. Additionally, the shape metrics indicate increasing compactness in the western Caribbean and eastern Gulf of Mexico, while decreasing compactness is more common in the western Gulf of Mexico and prior to landfall over the Greater Antilles islands and Yucatan Peninsula.

As TCs on a westward trajectory approach landfall, the results depict a striking increase in asymmetry and fragmentation (Figure 8A-B), particularly for landfalls in the western Gulf of Mexico. In contrast, for TCs that move north- and northeast-ward across the Gulf of Mexico and make landfall in the panhandle and Big Bend regions of Florida (e.g. Tropical Storm (TS) Debby (2012)), we observe increases in symmetry and cohesiveness in the approach to landfall. Lastly, precipitation disperses (Figure 8C) from the TC center across the majority of the region, although an area of decreased dispersiveness exists in the central Gulf of Mexico. This decrease appears to be short-lived as the TCs presumably move into a less favorable environment characterized by strong vertical wind shear and reduced latent and sensible heat fluxes over land.

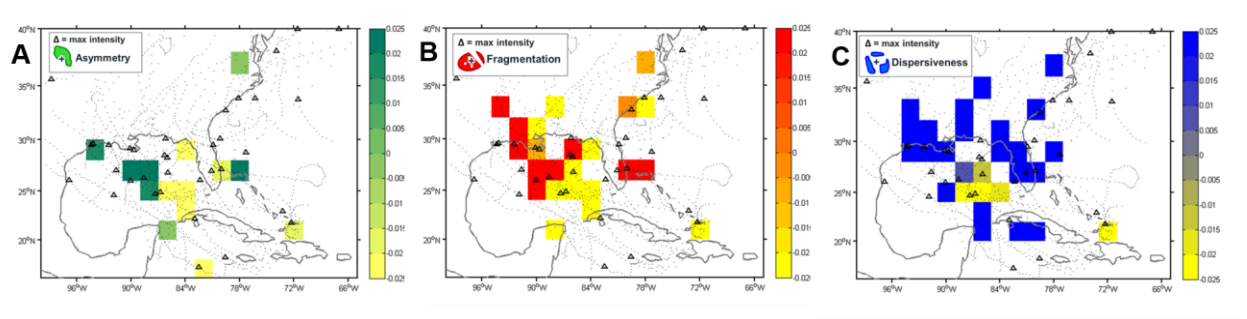

Figure 8 Average shape metric trends within 2.5° × 2.5° latitude-longitude grid boxes, calculated by averaging 3-hourly positions when Mann Whitney *U*-test indicates a significantly ($p < 0.05$) evolving pattern.

5. CONCLUSIONS

In this study, we outline a method for evaluating structural changes in synoptic-scale TC precipitation. By quantifying shape, rather than summarizing the pattern qualitatively, we develop a robust technique for analyzing storm-scale changes in TC rainfall. This geospatial method involves three shape metrics that characterize TC precipitation patterns ranging from highly compact (in intense TCs) to asymmetric, fragmented, and dispersed from the TC center (in TCs that are weak, dissipating, or transitioning into extratropical systems). We formulate three specialized shape metrics to quantify the two-dimensional pattern of precipitation signatures. These three metrics are variations on the theme of compactness, and collectively, the metrics characterize observed changes in structure during dissipation and/or extratropical transition as TCs move into the mid-latitudes. We then apply a moving Mann-Whitney *U* test to determine time periods in which the shape metrics indicate significant structural changes.

First, the methods are demonstrated with a case study of Hurricane Katrina. By tying the synoptic-scale precipitation pattern to internal and external controls of TC structure, we exhibit how this technique may be utilized to identify significant evolutionary periods. Next, we extend the shape metric methodology to all 2004-2012 U.S. landfalling TCs. A spatial depiction of increasing versus decreasing tropical structure indicates that TCs display statistically significant ($p < 0.05$) increases in compactness in the southern, central, and eastern Gulf of Mexico. Additionally, significant increases in asymmetry, fragmentation, and dispersiveness occur in the western Gulf of Mexico during a window of time that precedes landfall. Future work will investigate the environmental factors that foster increased (decreased) compactness in the eastern (western) Gulf of Mexico.

Based on this research, geospatial methods are useful for measuring the spatial evolution of TC precipitation. We expect that this methodology will facilitate the identification of dynamic and thermodynamic processes that influence synoptic-scale precipitation structure. Furthermore, shape methods may be useful in studying other weather phenomena that organize into characteristic geometries (e.g., bow echoes, supercells). In the present analysis, there are a few limitations to consider. First, we utilize accumulated 3-hour precipitation output from a 32-km reanalysis that must parameterize sub-gridscale eyewall processes, and thus, we recommend verifying the results with observational datasets. Second, we focus on the synoptic-scale precipitation pattern rather than the actual rain rate, which must be considered when forecasting the highest rainfall totals. Future work will use radar and satellite datasets to investigate smaller-scale embedded features within the broader precipitation pattern to quantify changes in high rain rate regions.

For forecasting implications, in Hurricane Katrina we reveal that increases in asymmetry, fragmentation, and dispersiveness are observed 6 hours (24 hours) prior to the timing of peak intensity (landfall). Results from 2004-2012 TCs indicate similar structural evolutions for storms moving across the western Gulf of Mexico in the approach to landfall. Thus, this methodology, derived from the geographic study of shape, shows promise in forecasting structural changes and, potentially, intensity changes when the large-scale environment impacts inner core dynamics. We expect that this study's research methods may be used to develop forecasting tools that 1) examine the degree of realism in an operational weather model's TC precipitation structures, as compared with satellite- and radar-derived rainfall and 2) aid in the creation of new TC rainfall models that do not rely so heavily on numerical weather prediction models and/or persistence. With improved forecasts and warning systems, it is hoped that fatalities resulting from extreme TC rainfall can be greatly reduced.

6. REFERENCES

Abarca, S. F., and K. L. Corbosiero, 2011: Secondary eyewall formation in WRF simulations of Hurricanes Rita and Katrina (2005). *Geophys. Res. Lett.*, **38**, L07802.

AghaKouchak, A., N. Nasrollahi, J. Li, B. Imam, and S. Sorooshian, 2011: Geometrical Characterization of Precipitation Patterns. *J. Hydrometeorol.*, **12**, 274–285.

Angel, S., J. Parent, and D. L. Civco, 2010: Ten compactness properties of circles: measuring shape in geography. *Can. Geogr. Géographe Can.*, **54**, 441–461.

Becker, E. J., E. H. Berbery, and R. W. Higgins, 2009: Understanding the Characteristics of Daily Precipitation over the United States Using the North American Regional Reanalysis. *J. Clim.*, **22**, 6268–6286.

Bukovsky, M. S., and D. J. Karoly, 2007: A brief evaluation of precipitation from the North American Regional Reanalysis. *J. Hydrometeorol.*, **8**, 837–846.

Chen, S. S., J. A. Knaff, and F. D. Marks Jr., 2006: Effects of Vertical Wind Shear and Storm Motion on Tropical Cyclone Rainfall Asymmetries Deduced from TRMM. *Mon. Weather Rev.*, **134**, 3190–3208.

Didlake, A. C., and R. A. Houze, 2009: Convective-Scale Downdrafts in the Principal Rainband of Hurricane Katrina (2005). *Mon. Weather Rev.*, **137**, 3269–3293.

DiMego, G. J., and L. F. Bosart, 1982: The Transformation of Tropical Storm Agnes into an Extratropical Cyclone. Part I: The Observed Fields and Vertical Motion Computations. *Mon. Weather Rev.*, **110**, 385–411.

Dvorak, V. F., 1975: Tropical Cyclone Intensity Analysis and Forecasting from Satellite Imagery. *Mon. Weather Rev.*, **103**, 420–430.

Elsberry, R. L., 2002: Predicting Hurricane Landfall Precipitation: Optimistic and Pessimistic Views from the Symposium on Precipitation Extremes. *Bull. Am. Meteorol. Soc.*, **88**, 47-64.

Foley, G. R., and B. N. Hanstrum, 1994: The Capture of Tropical Cyclones by Cold Fronts off the West Coast of Australia. *Weather Forecast.*, **9**, 577–592.

Frolov, Y. S., 1975: Measuring the Shape of Geographical Phenomena: A History of the Issue. *Sov. Geogr.*, **16**, 676–687.

Gray, W. M., 1968: Global View of the Origins of Tropical Disturbances and Storms. *Mon. Weather Rev.*, **96**, 669–700.

Hart, R. E., and J. L. Evans, 2001: A Climatology of the Extratropical Transition of Atlantic Tropical Cyclones. *J. Clim.*, **14**, 546–564.

Hence, D. A., and R. A. Houze Jr., 2008: Kinematic structure of convective-scale elements in the rainbands of Hurricanes Katrina and Rita (2005). *J. Geophys. Res.-Atmospheres*, **113**, D15108.

Hendricks, E. A., M. T. Montgomery, and C. A. Davis, 2004: The Role of "Vortical" Hot Towers in the Formation of Tropical Cyclone Diana (1984). *J. Atmospheric Sci.*, **61**, 1209–1232.

Jagger, T. H., and J. B. Elsner, 2006: Climatology models for extreme hurricane winds near the United States. *J. Clim.*, **19**, 3220–3236.

Jin, Y., M. S. Peng, and H. Jin, 2008: Simulating the formation of Hurricane Katrina (2005). *Geophys. Res. Lett.*, **35**, L11802.

Jones, S. C., and Coauthors, 2003: The extratropical transition of tropical cyclones: Forecast challenges, current understanding, and future directions. *Weather Forecast.*, **18**, 1052-1092.

Kaplan, J., and M. DeMaria, 2003: Large-Scale Characteristics of Rapidly Intensifying Tropical Cyclones in the North Atlantic Basin. *Weather Forecast.*, **18**, 1093–1108.

Klein, P. M., P. A. Harr, and R. L. Elsberry, 2000: Extratropical Transition of Western North Pacific Tropical Cyclones: An Overview and Conceptual Model of the Transformation Stage. *Weather Forecast.*, **15**, 373–395.

Knabb, R. D., J. R. Rhome, and D. P. Brown, 2005: *Tropical cyclone report: Hurricane Katrina, 23-30 August 2005*. National Hurricane Center,.

Knaff, J. A., D. P. Brown, J. Courtney, G. M. Gallina, and J. L. Beven, 2010: An Evaluation of Dvorak Technique–Based Tropical Cyclone Intensity Estimates. *Weather Forecast.*, **25**, 1362–1379.

Lin, Y., K. Mitchell, E. Rogers, M. Baldwin, and G. DiMego, 1999: Test assimilations of the real-time, multi-sensor hourly precipitation analysis into the NCEP Eta model. Preprints, 8th Conf. on Mesoscale Meteorology, Boulder, CO, Amer. Meteor. Soc, 341–344.

Li, W., M. F. Goodchild, and R. Church, 2013: An efficient measure of compactness for two-dimensional shapes and its application in regionalization problems. *Int. J. Geogr. Inf. Sci.*, **27**, 1227–1250.

——, T. Chen, E. A. Wentz, and C. Fan, 2014: NMMI: A Mass Compactness Measure for Spatial Pattern Analysis of Areal Features. *Ann. Assoc. Am. Geogr.*, **104**, 1116–1133.

MacEachren, A. M., 1985: Compactness of Geographic Shape: Comparison and Evaluation of Measures. *Geogr. Ann. Ser. B Hum. Geogr.*, **67**, 53–67.

Malmquist, D. L., 1999: Meteorologists and insurers explore extratropical transition of tropical cyclones. *Eos Trans. Am. Geophys. Union*, **80**, 79–80.

Matyas, C., 2007: Quantifying the Shapes of U.S. Landfalling Tropical Cyclone Rain Shields*. *Prof. Geogr.*, **59**, 158–172.

——, 2008: Shape measures of rain shields as indicators of changing environmental conditions in a landfalling tropical storm. *Meteorol. Appl.*, **15**, 259–271.

——, 2009: A Spatial Analysis of Radar Reflectivity Regions within Hurricane Charley (2004). *J. Appl. Meteorol. Climatol.*, **48**, 130-142.

McTaggart-Cowan, R., L. F. Bosart, J. R. Gyakum, and E. H. Atallah, 2007: Hurricane Katrina (2005). Part I: Complex Life Cycle of an Intense Tropical Cyclone. *Mon. Weather Rev.*, **135**, 3905–3926.

Mesinger, F., and Coauthors, 2006: North American regional reanalysis. *Bull. Am. Meteorol. Soc.*, **87**, 343–360.

Rappaport, E. N., and Coauthors, 2009: Advances and Challenges at the National Hurricane Center. *Weather Forecast.*, **24**, 395-419.

Riemer, M., and M. T. Montgomery, 2011: Simple kinematic models for the environmental interaction of tropical cyclones in vertical wind shear. *Atmos Chem Phys*, **11**, 9395–9414.

Rogers, R., F. Marks, and T. Marchok, 2009: Tropical Cyclone Rainfall. *Encyclopedia of Hydrological Sciences*, John Wiley & Sons, Ltd.

Royer, A., and S. Poirier, 2010: Surface temperature spatial and temporal variations in North America from homogenized satellite SMMR-SSM/I microwave measurements and reanalysis for 1979–2008. *J. Geophys. Res. Atmospheres*, **115**, D80110.

Ruane, A. C., 2010a: NARR's atmospheric water cycle components. Part I: 20-year mean and annual interactions. *J. Hydrometeorol.*, **11**, 1205–1219.

——, 2010b: NARR's atmospheric water cycle components. Part II: Summertime mean and diurnal interactions. *J. Hydrometeorol.*, **11**, 1220–1233.

Schenkel, B. A., and R. E. Hart, 2012: An Examination of Tropical Cyclone Position, Intensity, and Intensity Life Cycle within Atmospheric Reanalysis Datasets. *J. Clim.*, **25**, 3453–3475.

Schwartzberg, J. E., 1965: Reapportionment, Gerrymanders, and the Notion of Compactness. *Minn. Law Rev.*, **50**, 443.

Shimazu, Y., 1998: Classification of Precipitation Systems in Mature and Early Weakening Stages of Typhoons around Japan. *J. Meteorol. Soc. Jpn. Ser II*, **76**, 437–445.

Simpson, J., E. Ritchie, G. J. Holland, J. Halverson, and S. Stewart, 1997: Mesoscale Interactions in Tropical Cyclone Genesis. *Mon. Weather Rev.*, **125**, 2643–2661.

Torn, R. D., and G. J. Hakim, 2009: Ensemble Data Assimilation Applied to RAINEX Observations of Hurricane Katrina (2005). *Mon. Weather Rev.*, **137**, 2817–2829.

Velden, C. S., T. L. Olander, and R. M. Zehr, 1998: Development of an objective scheme to estimate tropical cyclone intensity from digital geostationary satellite infrared imagery. *Weather Forecast.*, **13**, 172-186.

Wentz, E. A., 1997: Shape analysis in GIS. Vol. 13 of, Proceedings of Auto-Carto, 204–213.

Wilcoxon, F., 1945: Individual comparisons by ranking methods. *Biom. Bull.*, **1**, 80–83.

Zick, S. E., and C. J. Matyas, 2015a: Tropical cyclones in the North American Regional Reanalysis: The impact of satellite-derived precipitation over-ocean. *J. Geophys. Res. Atmospheres*, **120,** 8724-8742.

——, and ——, 2015b: Tropical cyclones in the North American Regional Reanalysis: An assessment of spatial biases in location, intensity, and structure. *J. Geophys. Res. Atmospheres*, **120**, 1651-1669.

——, and ——: A shape metric methodology for studying the evolving geometries of synoptic-scale precipitation patterns in tropical cyclones. *Annals of the Association of American Geographers*, Submitted Nov, 11, 2015.